Juxtacanalicular Tissue in Pigmentary and Primary Open Angle Glaucoma

The Hydrodynamic Role of Pigment and Other Constituents

Collin G. Murphy, PhD; Mark Johnson, PhD; Jorge A. Alvarado, MD

• **We tested the hypothesis that obstruction of the juxtacanalicular tissues, by melanin granules in pigmentary glaucoma and by other impermeable material in primary open angle glaucoma, leads to the development of a chronic glaucomatous condition. The distribution and concentration of melanin and other impermeable materials in the juxtacanalicular tissues and elsewhere in the trabecular meshwork was determined in 13 specimens. Six specimens were from patients with pigmentary glaucoma, two from patients with pigment dispersion syndrome, and three from patients with primary open angle glaucoma, as well as two from normal subjects. The effect of these materials on flow resistance was estimated using two hydrodynamic models. In model A, the electron-lucent spaces of the juxtacanalicular tissue were assumed to be open spaces, while in model B, these spaces and spaces filled with ground substance were assumed to be gel filled. In pigmentary glaucoma, 3.5% of the pigment was found in the juxtacanalicular tissue, while 96.5% was found in the corneoscleral and uveoscleral tissues. Permeabilities calculated according to model A were much higher than those expected from estimates of outflow facility in all groups, in agreement with the previous report of Ethier et al. The gel-filled spaces available for fluid flow, as determined by model B, showed no statistically demonstrable differences (pigmentary glaucoma, 32.9%; primary open angle glaucoma, 36.6%; pigment dispersion syndrome, 43.4%; normal, 44.1%). Furthermore, the amount of pigment present in the juxtacanalicular tissue was determined to have a negligible influence on permeability. Thus, the development of the chronic glaucomatous condition cannot be directly attributed to pigment accumulation in the juxtacanalicular tissue in pigmentary glaucoma.**

(*Arch Ophthalmol.* 1992;110:1779-1785)

Deposition of melanin granules within the trabecular tissues has been associated with a short-term or even a long-term elevation of the intraocular pressure (IOP).[1] The short-term pressure rise seems to be produced by the sudden obstruction of aqueous outflow as demonstrated experimentally in perfusion studies.[1-4] These intermittent elevations of pressure are also observed clinically when pigment is released following either pupillary dilation or vigorous exercise in susceptible persons.[5-8] How pigment accumulation leads to the development of chronic IOP elevation and pigmentary glaucoma (PG) is unclear. It has been proposed that melanin granules become trapped at the level of the juxtacanalicular tissue (JXT), leading to the permanent obstruction of aqueous outflow.[9] This process would be analogous to the plugging of a kitchen sink by coffee grounds. However, histologic studies have shown that surprisingly few melanin granules are in the JXT and have not identified other obstruction sites.[10-16]

See also p 1769.

Morphometric methods have been used in conjunction with porous media theory to estimate the amount of flow resistance generated by the content of materials with low permeability in the JXT. Such methods have suggested (in one eye) that in patients with PG there is a higher resistance compared with patients with primary open angle glaucoma (POAG) and normal subjects.[17] This observation raised the possibility that deposited pigment granules reduce the space occupied by the highly conducting or more "porous" structures of the JXT. To test this hypothesis, we first measured the content of melanin granules within the JXT (and the other trabecular meshwork [TM] layers) and then calculated how the JXT permeability might be altered in PG and POAG.

Our measurements do not support the idea that melanin granules are preferentially trapped in the JXT, as most of the pigment particles in PG specimens are found upstream in the uveoscleral (UVM) and corneoscleral (CSM) meshworks. We find little evidence to support the hypothesis that an obstruction by melanin or other materials with low permeability leads to an alteration of the JXT permeability and produces the chronic glaucomatous condition in PG or in POAG. However, these studies do provide a broader verification of the conclusion of Ethier et al[17] and Seiler and Wollensak[18] that the electron-lucent spaces found in the JXT must be gel filled to generate a significant flow resistance.

MATERIALS AND METHODS

Specimen Collection and Preparation

Thirteen specimens were collected for this study (Table 1). Six specimens from patients with PG were obtained at trabeculectomy and fixed within seconds after excision. These specimens were especially dissected to ensure that the entire outflow pathway and the iris root were included in each tissue block (Fig 1). The only exception is specimen 0186, which was missing a portion of the UVM. Two pairs of eyes from patients with pigment dispersion syndrome (PDS) without glaucoma (ie, normal IOP and outflow facility) were also analyzed. One pair was obtained and fixed immediately after death and the other was obtained and fixed 12 hours post mortem.

Three age-matched specimens from patients with POAG included one promptly fixed trabeculectomy specimen and two pairs of eyes fixed within 4 hours post mortem. Two age-matched pairs of eyes from nonglaucomatous normal subjects (NL), fixed 4 hours post mortem, served as controls. Patient ages, IOPs, and medications are listed in Table 1. Informed consent was obtained, before undertaking this study, from patients or relatives according to standard methods. None of the specimens had received prior laser treatment, with the exception of case 1362, in which one meshwork quadrant, 180° from the trabeculectomy site, had been treated with the argon laser instrument. Tissues were fixed, dehydrated,

Accepted for publication June 11, 1992.

From the Department of Ophthalmology, Glaucoma Research Laboratory, University of California School of Medicine, San Francisco (Drs Murphy and Alvarado); and the Department of Mechanical Engineering, Massachusetts Institute of Technology, Cambridge (Dr Johnson).

Presented in part at the annual meeting of the Association for Research in Vision and Ophthalmology, Sarasota, Fla, May 3, 1990.

Reprint requests to Department of Ophthalmology, Box 0730, University of California School of Medicine, San Francisco, CA 94143 (Dr Alvarado).

Table 1.—Clinical Findings and Specimen Characteristics*

Diagnostic Group	Patient Age, y/ Sex	Medications†	Specimen No.	Intraocular Pressure, mm Hg	Specimen Source
PG	23/M	Epinephrine hydrochloride, timolol maleate, pilocarpine nitrate, acetazolamide	0169	30	T
			0186	30	T
	64/F	Timolol, pilocarpine, acetazolamide	0834	44	T
	67/M	Epinephrine, timolol, pilocarpine, acetazolamide	1243	33	T
			1314	30	T
	68/M	Epinephrine, pilocarpine, acetazolamide, betaxolol hydrochloride	1362	37	T
PDS	30/F	...	0619	13	Eyes
	67/M	Epinephrine, timolol	0845	18.8 (±3.3)	Eyes
POAG	62/F	Pilocarpine	0977	26	T
	62/M	Pilocarpine, acetazolamide, betaxolol, methazolamide	1335	27	T
	71/M	Epinephrine, pilocarpine, acetazolamide, echothiophate iodide	0612 OU	32	Eyes
NL eyes	64/M	...	0406	...	Eyes
	69/M	...	0127	...	Eyes

*Intraocular pressure indicates highest recorded; PG, pigmentary glaucoma; T, trabeculectomy; PDS, pigment dispersion syndrome; POAG, primary open angle glaucoma; and NL, normal nonglaucomatous. For specimen 0845, intraocular pressures measured during a 19-year period were averaged. This patient had a facility of outflow of 0.24, and no visual field defects or disc changes were observed during this time.

†Medications include all of those used during the course of treatment.

embedded, and sectioned as described in a previous report.[19]

Morphometry

Only the portion of the JXT internal to Schlemm's canal was considered; this region was defined as the connective tissue limited internally by the outermost aqueous channels or intertrabecular spaces, externally by the endothelium of the inner wall of Schlemm's canal, and anteriorly and posteriorly by the corresponding margins of Schlemm's canal.[19] Meridional tissue sections of the JXT were photographed in a series of contiguous micrographs that were then assembled into a montage representing the entire structure (×6500).

The montage was divided into segments at approximately 30-μm intervals along its anteroposterior axis (five to 10 such segments for each specimen). The area of each segment, its open spaces (model A; see below), and constituents (model B; see below) were traced to make the desired measurements (Fig 2). To describe the structure of the JXT in greater detail, its average thickness (mean of means) was determined from measurements taken at 3-μm intervals.

The pigment content was assessed by measuring its distribution and concentration within three regions of the TM (JXT, CSM, and UVM). Pigment distribution was determined by first measuring the aggregate area occupied by both intracellular and extracellular melanin granules in the entire TM. Then, the percentage of that area found in each region was used to describe pigment distribution. Pigment concentration in each region was determined by dividing the area occupied by melanin granules in a specified region by the area of that tissue. For the JXT, the electron micrograph montages described earlier were used, and for the CSM and UVM, we used montages of light micrographs (magnification, ×1700) made from meridional sections of specimens from patients with PG and PDS. (Morphometric measurements were carried out on a Summagraphics digitizing pad [Fairfield, Conn] interfaced with an IBM XT personal computer.) So few melanin granules occurred in the CSM and UVM of POAG and NL specimens that we did not measure their area.

Permeability Models

Two hydrodynamic models of the JXT, as described by Ethier et al,[17] were used to characterize its hydrodynamic properties. In model A, the electron-lucent spaces in the JXT (Fig 2, top) were considered to be open spaces available for flow. For calculations with this model, the areas and perimeters of individual electron-lucent spaces in the JXT were traced on each segment. Then, we calculated porosity, specific surface, and hydrodynamic permeability in two specimens from each diagnostic group (eight eyes). *Porosity* (ϵ, calculated as "pore" volume per unit volume) was defined as the ratio of the sum of the electron-lucent areas in the JXT to the total JXT area. Similarly, *specific surface* (S, calculated as pore surface area per unit volume) was determined as the ratio of the sum of the perimeters of the electron-lucent spaces to the total JXT area. *Hydrodynamic permeability* (K, expressed in square centimeters) was then determined by the Carman-Kozeny equation: $K=\epsilon^3/4S^2$.[17] A related value, the hydraulic radius ($2\epsilon/S$), characterizing the average size of openings in the JXT, was also calculated.

In model B, the electron-lucent spaces and other spaces filled with a light gray, amorphous, gel-like material (ground substance) are considered to be filled with a homogeneous gel and available for flow. For calculations with this model, the areas occupied by impermeable JXT constituents were traced on each segment (Fig 2, middle, bottom). The fractions of each segment occupied by melanin (intracellular and extracellular), plaque material,[19] collagen (fibrils and bundles), and cells were calculated. These measurements were made in 13 specimens. The aggregate area of impermeable material was then divided by the total JXT area to yield the impermeable fraction or proportion of this tissue occupied by impermeable structures. The remaining tissue is defined as the JXT area occupied by a gel, or the gel fraction. As an indicator of tissue hydrodynamic permeability, we compared the gel fraction among the diagnostic categories. To determine how pigment accumulation affected the gel fraction, we calculated how this fraction would have increased by removal of both intracellular and extracellular pigment. Then we could determine the direct, porosity-decreasing effect of pigment on flow resistance.

The fractional increase in flow resistance (ΔR) due to accumulated pigment was found as follows:

$$\Delta R=(A_0/A_{gel})-1=(A_{icp}+A_{ecp})/A_{gel},$$

where A_{gel} indicates gel fraction; A_{icp}, intracellular pigment; A_{ecp}, extracellular pigment; and $A_0=A_{gel}+A_{icp}+A_{ecp}$. Implicit in this equation is the assumption that the extracellular matrix permeability in the gel-filled spaces is the same with or without pigment, consistent with the hypothesis that we are examining, namely, that pigment affects outflow resistance by directly decreasing the open space available for flow.

Mean values for each of the variables measured in the two models were obtained using data from the entire JXT region. The values for the individual segments were used to calculate an SE for each specimen.

RESULTS

Pigment Distribution and Concentration

Inspection of Table 2 shows large and statistically significant differences in pigment distribution among the tissue regions. In PG, most of the pigment (96.5%) is found internal to the JXT in the CSM and UVM meshworks. Only a minor portion (3.5%) of the pigment is actually present in the JXT. Table 2 shows that regional differences in pigment concentration, however, are less striking, but still statistically demonstrable. The JXT has an average concentration of 1.3% compared with 3.9% and 2.3% in the CSM and UVM, respectively. In comparing PDS with PG, it is difficult to determine whether there are any real differences in pigment distribution, concentration, or the total amount of pigment in the TM. The small differences observed in Table 2 are not statistically significant.

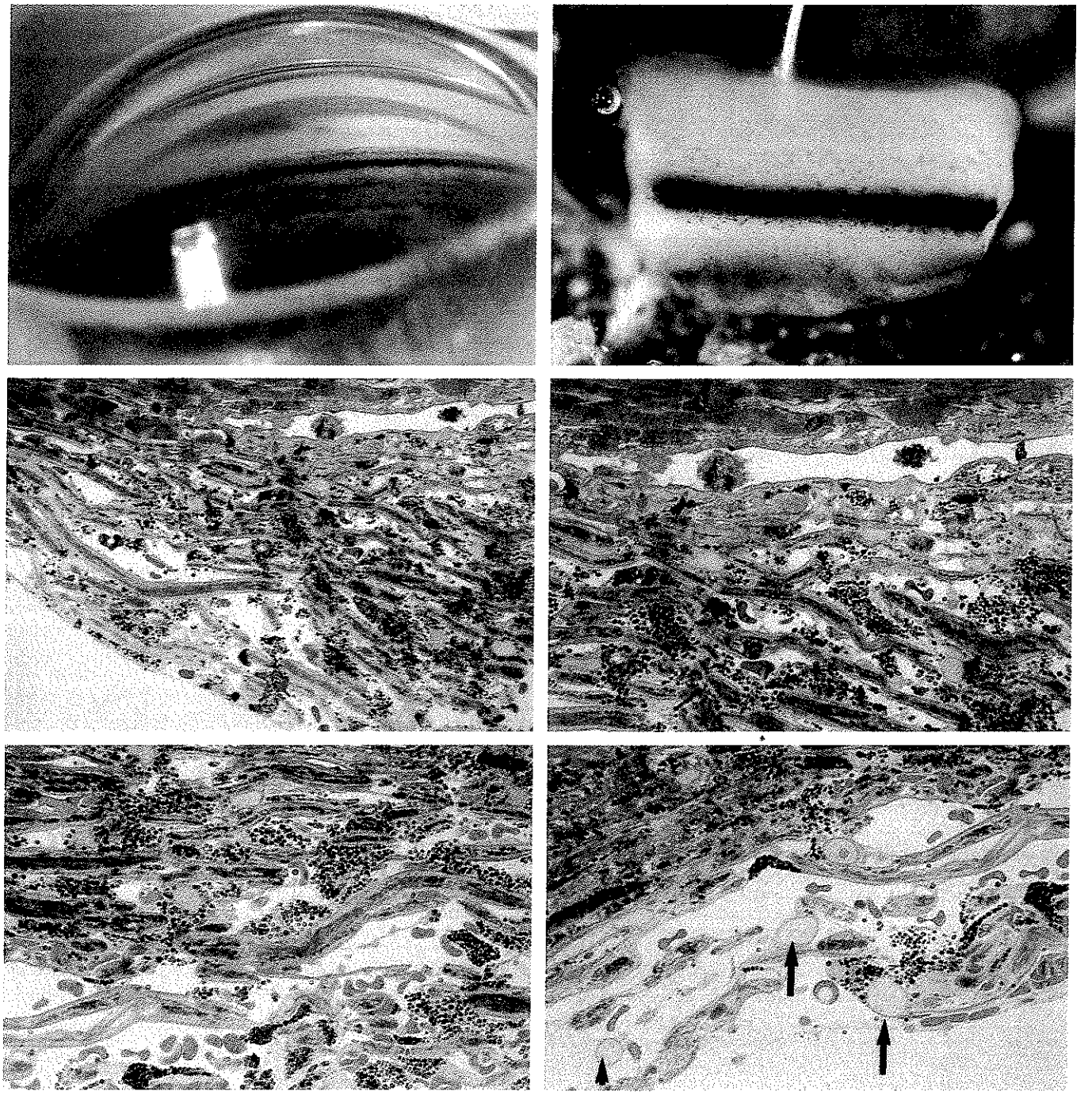

Fig 1.—Severe case of pigmentary glaucoma in a 62-year-old man. Top left, Goniophotograph. Note intense trabecular pigmentation and Krukenberg spindle on the cornea. Top right, Trabeculectomy specimen (No. 1362) from the same patient. A black band of tissues has been created by the deposited pigment granules. The entire outflow pathway is included in the specimen. Note the ciliary body band, iris root, filtration zone, etc (×200). Light micrographs of meridional sections of this specimen are shown at center and bottom parts of this figure. Center left, Pigment deposited in the trabecular meshwork is most concentrated in the uveal and corneoscleral tissues (×600). Center right, Higher magnification. Note relative lack of pigment accumulation in the juxtacanalicular tissue region (arrows) (×800). Bottom left, Abundant pigment in corneoscleral and uveoscleral meshworks (×600). Bottom right, Rounded nuclei (arrows) indicate necrotic cells in the uveal meshwork (toluidine blue, ×600).

Permeability Models

The permeability values of the JXT of the eight specimens calculated using model A are given in Table 3. Relative values are ordered as might be expected for the diagnoses. The highest calculated hydrodynamic permeability was obtained in NL specimens (mean $K=60.3\times10^{-12}$ cm^2) and the lowest was obtained in POAG specimens (mean $K=3.25\times10^{-12}$ cm^2). Intermediate values were obtained for the PDS specimens (mean $K=9.3\times10^{-12}$ cm^2) and PG specimens (mean $K=18.5\times10^{-12}$ cm^2). However, all of these values were much greater than the known typical values of the normal (0.35×10^{-12} cm^2) or glaucomatous (0.06 to 0.11×10^{-12} cm^2) outflow pathway (see "Comment" for details), in substantial agreement with the findings of Ethier et al.[17]

Porosity and hydraulic radius measurements also seem to be ordered according to expectations, as with the

Fig 2.—A portion of Schlemm's canal (SC) and juxtacanalicular tissue (JXT) is shown at the magnification (uranyl acetate–lead citrate, ×6500) used to make the measurements (specimen 845). Top, The JXT (outlined by dotted line) extends between the inner wall (IW) endothelium lining SC and the trabecular cells (TC) lining the outermost aqueous channels of the trabecular meshwork. Electron-lucent spaces (hatched regions) were outlined to determine their areas and perimeters for the porosity and permeability calculations according to model A. Center, For model B, the areas occupied by several types of impermeable components were measured. Here, plaque material (hatched areas) is indicated on the same micrograph as at top. Bottom, Additional materials measured for model B included areas occupied by cellular material (blackened areas), collagen (hatched areas), and melanin granules (not shown). To determine the gel fraction, the areas of plaque, cells, collagen, and melanin were subtracted from the total JXT area.

permeability calculations (Table 3). The thickness of the JXT is highly variable, with no clear differences among diagnostic groups (Table 4).

The fractions for various low-permeability constituents of the JXT and the permeable gel-filled spaces calculated according to model B for 13 specimens are given in Table 5. Again, as seen for model A, the relative values for the fraction of permeable spaces were ordered as might be expected among the diagnostic categories; ie, NL and PDS specimens had higher average gel fractions (0.44 and 0.43) than did PG and POAG specimens (0.33 and 0.37). However, there was a large variability within categories, and no statistically discernible difference could be found for this or any of the other constituent fractions measured. The gel fraction data indicate that on the average, 40% (measured range, 22% to 50%) of the JXT tissue is actually occupied by permeable spaces.

There seemed to be somewhat more pigment in the JXT in PG (1.0%) and PDS (0.7%) than in POAG (0.2%) and NL (0.15%) specimens, but the number of specimens was too small to demonstrate statistical significance. The fractional increase in flow resistance due to pigment was small in all groups, and averaged only 0.9% in PG.

COMMENT

The main focus of our investigation was to test the hypothesis that a buildup of pigment in the JXT region might obstruct aqueous outflow and contribute to the elevated flow resistance characteristic of PG. Distribution studies indicate that the preponderance of pigment granules are trapped upstream of the JXT. These findings agree with previous qualitative observations as reported by others.[10-16] Even in the specimen (No. 1362, Fig 1) that had six times more pigment than the others, only 7.5% of its pigment was in the JXT. Buildup of pigment in the UVM and CSM would result from an "upstream" capture of this particulate matter before it reaches the JXT. This mechanism has been demonstrated in an experimental model[20] and would be expected, since trabecular cells are avid phagocytes.[21] Our studies indicate that approximately 1% of the JXT is occupied by melanin. Whether this amount of pigment would be sufficient to play a major role in outflow obstruction was ascertained by comparison of calculated hydrodynamic properties of the JXT in PG and the other diagnostic categories.

The JXT permeabilities calculated using model A, in which only the electron-lucent spaces in the JXT are presumed to be available for fluid flow, indicate no significant differences among the diagnostic categories, even though the trends were in the direction expected. Outweighing any such trends is the striking fact that all of the calculated permeabilities are much too high compared with the expected values.

Table 2.—Pigment Distribution and Concentration in PG and PDS*

Diagnostic Group, Specimen No.	Pigment Distribution (% of Total Pigment)			Pigment Concentration (% of Tissue Area)		
	JXT	CSM	UVM	JXT	CSM	UVM
PG						
0169	4.5	80.0	15.5	0.2	0.5	0.2
0834	1.0	46.8	52.2	0.6	1.8	1.4
1243	1.3	27.5	71.3	0.4	3.7	1.0
1314	3.4	48.0	48.6	1.1	1.6	1.1
1362	7.5	62.5	30.0	4.0	12.0	7.8
Mean±SE	3.5±1.2	53.0±8.7	43.5±9.6	1.3±0.7	3.9±2.0	2.3±1.3
PDS						
0619	0.3	50.0	49.7	1.2	10.4	19.0
0845	1.2	52.1	46.7	0.2	1.5	1.1
Mean±SE	0.8±0.5	51.0±1.0	48.2±1.5	0.7±0.5	6.0±4.5	10.1±8.6

*PG indicates pigmentary glaucoma; PDS, pigment dispersion syndrome; JXT, juxtacanalicular tissue; CSM, corneoscleral meshwork; and UVM, uveoscleral meshwork. Pigment distribution is shown as the percentage of pigment found within the three meshwork regions in each specimen. Pigment concentration is shown as the percent of tissue area occupied by pigment in each specimen region. Regional differences in distribution of pigment are significant (one-tailed, paired *t* tests). For PG, JXT vs CSM, $P<.001$; JXT vs UVM, $P<.01$; for PDS, JXT vs CSM, $P<.005$; JXT vs UVM, $P<.02$. Regional differences in concentration are significant when the JXT and CSM are compared in all seven specimens (one-tailed, paired *t* test, $P<.05$), while other comparisons are of borderline significance ($P\cong.1$).

Table 3.—Determination of Hydrodynamic Permeability and Hydraulic Radius of JXT Region Using Model A*

Diagnostic Group, Specimen No.	Porosity	Permeability, $cm^2\times10^{-12}$	Hydraulic Radius, μm
PG			
1243	0.125±0.026	5.7±2.1	0.27±0.02
1362	0.181±0.010	31.3±6.6	0.53±0.04
PDS			
0619	0.106±0.029	6.8±4.4	0.32±0.05
0845	0.129±0.019	11.8±8.8	0.38±0.02
POAG			
1335	0.051±0.023	2.9±12.7	0.30±0.09
0612	0.065±0.008	3.4±0.7	0.29±0.02
Normal			
0406	0.143±0.014	20.4±4.8	0.48±0.03
0127	0.259±0.023	100.3±29.5	0.79±0.09

*JXT indicates juxtacanalicular tissue; PG, pigmentary glaucoma; PDS, pigment dispersion syndrome; and POAG, primary open angle glaucoma. Values are mean±SE. For reference, the estimated permeability of the aqueous outflow system (see text) is approximately 0.35×10^{-12} cm^2 for normal subjects and ranges from 0.058 to 0.11×10^{-12} cm^2 for patients with glaucoma. See text for explanation of Model A.

Table 4.—Thickness of JXT, Measured From Outermost Aqueous Channels to Lining of Schlemm's Canal*

Diagnostic Group, Specimen No.	JXT Thickness, μm, Mean±SD
PG	
0169	9.00±1.88
0186	11.40±2.98
0834	6.39±0.42
1243	3.08±1.39
1314	8.97±4.5
1362	8.94±3.94
Mean±SD	7.96±2.87
PDS	
0619	4.22±1.97
0845	6.43±2.58
Mean±SD	5.33±1.56
POAG	
0977	8.99±2.79
1335	6.82±2.38
0612	7.59±4.39
Mean±SD	7.8±1.1
Normal	
0406	11.35±3.71
0127	6.57±2.94
Mean±SD	8.96±3.38

*JXT indicates juxtacanalicular tissue; PG, pigmentary glaucoma; PDS, pigment dispersion syndrome; and POAG, primary open angle glaucoma.

(For this computation, we have assumed that the entire pressure drop in the aqueous outflow pathway occurs across the JXT and have used known outflow facility values and Darcy's law: $\Delta P/Q=\mu L/KA$, where ΔP is the system pressure drop [~5-mm Hg pressure drop]; Q, the flow rate [~2 μL/min]; μ, the viscosity of the aqueous humor [0.72 centipose]; L, the distance across the JXT [10 μm][17]; and A, the cross-sectional area facing flow [0.11 cm^2].[22] For normal eyes, we used an IOP of 15 mm Hg and a 4–mm Hg pressure drop; for glaucomatous eyes, we used an IOP of 25 mm Hg [15-mm Hg pressure drop] or 40 mm Hg [30-mm Hg pressure drop]). The major outflow pathway or TM in normal eyes has a permeability of 0.35×10^{-12} cm^2. Our studies show that the JXT has a mean permeability in normal eyes of 60.3×10^{-12} cm^2, or about 200 times greater than that expected if a major portion of the resistance to aqueous outflow resides in the JXT. In glaucomatous eyes, the permeability for the outflow pathway ranges from about 0.11×10^{-12} cm^2 to 0.058×10^{-12} cm^2. The mean JXT permeability obtained for POAG specimens in this study is at least 30 times greater than the expected value, since it measures 3.25×10^{-12} cm^2. One conclusion from the use of model A is that the open spaces in the JXT are too large to generate a significant flow resistance unless they are gel filled, as pointed out by Ethier et al[17] and Seiler and Wollensak.[18]

Although some of the values used in our computations of expected JXT permeabilities may be inaccurate, it is unlikely that these discrepancies could account for the differences noted. For instance, we used a value of 0.11 cm^2 for the area of the JXT facing flow, in agreement with published values.[22] More recent measurements indicate that this value might be 25% smaller in POAG.[23] Such a reduction in area would simply result in a proportional increase in the permeability calculated using Darcy's law. Similarly, we used 10 μm as the JXT thickness, even though our data given in Table 3 indicate that this value may be somewhat lower (mean±SD, 7.7±2.5 μm). A thinner JXT would result in a proportional decrease in the estimated permeability. These corrections for area or thickness of the JXT would be minor compared with the differences (at least 30-fold) noted.

Ethier et al[17] suggested that model B, in which all spaces in the JXT not containing impermeable components are uniformly filled with a permeable extracellular matrix gel, provides a more pertinent depiction of the open spaces in the JXT. Therefore, we used model B to discover (1) whether the proportion of the JXT occupied by permeable spaces differs among the diagnostic groups, and (2) whether these differences might be related to the extent of pigment accumulation. We found that the differences in gel-filled, permeable spaces between the diagnostic groups were too small to account for the different outflow facilities of these groups. With regard to the effects of pigment accumulation, only a small fraction of the JXT was occupied by pigment, and the effect of pigment accumulation on flow resistance (as determined by the decrease of

Table 5.—Volume Fraction of Various JXT Constituents and Effect of Pigment on Flow Resistance (ΔR)*

Diagnostic Group, Specimen No.	Plaque	Collagen	Cellular	Melanin ($A_{ecp}+A_{icp}$)	Gel (A_{gel})	ΔR
PG						
0169	0.078±0.010	0.335±0.017	0.364±0.032	0.002±0.001	0.224±0.033	0.008±0.008
0186	0.058±0.017	0.306±0.029	0.413±0.037	0.002±0.002	0.222±0.037	0.008±0.013
0834	0.305±0.092	0.206±0.047	0.114±0.050	0.006±0.006	0.375±0.088	0.016±0.012
1243	0.218±0.030	0.218±0.050	0.129±0.023	0.004±0.007	0.431±0.043	0.009±0.017
1314	0.115±0.005	0.307±0.032	0.249±0.059	0.011±0.006	0.318±0.080	0.033±0.080
1362	0.226±0.022	0.119±0.027	0.244±0.026	0.040±0.007	0.404±0.031	0.100±0.021
Mean±SE	0.167±0.040	0.249±0.034	0.252±0.049	0.010±0.006	0.329±0.037	0.009±0.015
PDS						
0619	0.058±0.011	0.288±0.032	0.162±0.023	0.012±0.006	0.487±0.023	0.024±0.013
0845	0.096±0.018	0.334±0.037	0.187±0.019	0.002±0.002	0.382±0.028	0.006±0.004
Mean±SE	0.077±0.019	0.311±0.023	0.174±0.012	0.007±0.005	0.434±0.052	0.015±0.00
POAG						
0977	0.224±0.010	0.200±0.025	0.162±0.021	0.000±0.000	0.413±0.028	0.000±0.000
1335	0.105±0.013	0.175±0.023	0.291±0.020	0.002±0.001	0.429±0.030	0.005±0.002
0612	0.145±0.040	0.351±0.040	0.250±0.030	0.001±0.000	0.255±0.020	0.005±0.001
Mean±SE	0.158±0.035	0.242±0.055	0.234±0.038	0.002±0.000	0.366±0.056	0.003±0.002
Normal						
0406	0.212±0.018	0.245±0.035	0.157±0.020	0.000±0.000	0.387±0.033	0.000±0.000
0127	0.074±0.016	0.178±0.020	0.253±0.018	0.003±0.003	0.495±0.017	0.005±0.005
Mean±SE	0.143±0.069	0.212±0.034	0.205±0.048	0.0015±0.0015	0.441±0.054	0.0025±0.0025

*JXT indicates juxtacanalicular tissue; PG, pigmentary glaucoma; PDS, pigment dispersion syndrome; and POAG, primary open angle glaucoma. For explanation of A_{ecp}, A_{icp}, and A_{gel}, see text.

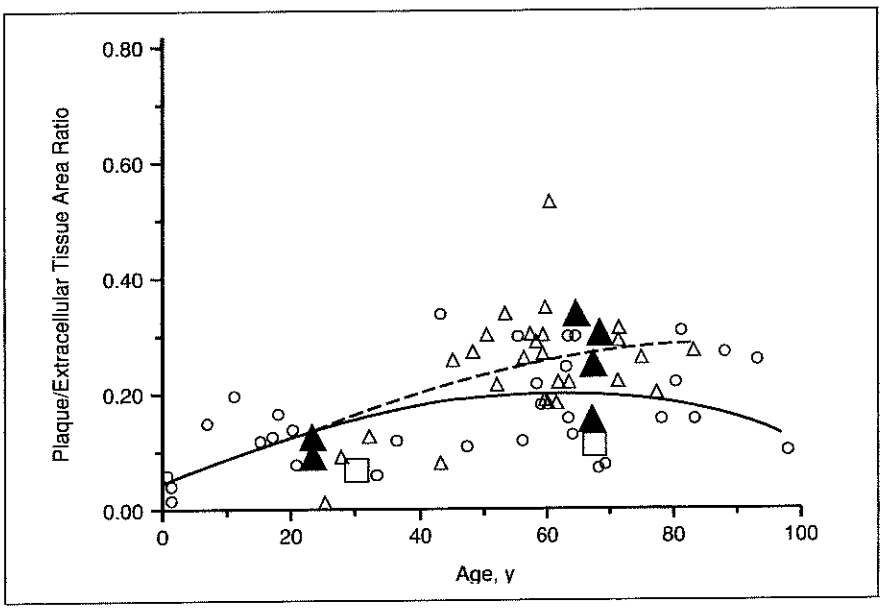

Fig 3.—Concentration of plaque material in the juxtacanalicular tissue (JXT) in six specimens from patients with pigmentary glaucoma (PG) (large triangles) and two from patients with pigment dispersion syndrome (PDS) (squares), compared with age-related regression curves described previously for 36 nonglaucomatous normal (NL) tissue specimens (circles) and 28 specimens from patients with primary open angle glaucoma (POAG) (small triangles).[19] Concentration of plaque is computed as Plaque Area/(JXT Tissue Area−Cellular Area). Before the approximate age of 45 years, there is a common regression line (solid line), which describes the age-related plaque accumulation in NL and POAG; thereafter, there is a slightly increased amount of plaque in POAG (broken line), so there are two gradually diverging curves. The two specimens obtained from the 23-year-old patient with PG (Nos. 0169 and 0186) are close to the common NL/POAG regression line. The other four PG specimens we examined were from patients in their middle to late 60s and are distributed across both regression lines. The PDS specimens have low amounts of plaque material.

available flow area) was negligible. Even in the eye with the largest accumulation of pigment (specimen 1362), the fractional increase in flow resistance due to pigment was estimated at 10%, which would increase the pressure difference across the aqueous outflow system from the usual 5.0 mm Hg to only 5.5 mm Hg, a change much too low to explain the chronic pressure elevation in PG. Thus, we conclude that neither hydrodynamic model can substantiate a basis for pigment directly obstructing outflow in PG.

The JXT is loosely organized compared with other ocular tissues. The JXT has a mean electron-lucent space content of 13% and a mean gel-filled fraction of about 40%. For comparison, corneal stromal lamella or Descemet's membrane would have zero electron-lucent space measured by the criterion of porosity in model A.[24] All specimens were fixed by immersion; fixation at a physiologic level of IOP would likely have increased the percentage of gel-filled space. It is also possible that hydrodynamic determinations made with these models are influenced by artifacts inherent in fixed, dehydrated tissue samples.

We considered plaque material as another possible source of obstruction as Rohen, Lütjen-Drecoll, and associates[25-29] had observed increased amounts of this substance in the JXT in POAG. These authors have thought that plaque accumulation could be responsible for an eventual blockage of certain preferential channels for aqueous flow. Use of model B indicates that plaque is not present in sufficient amounts to account for the outflow obstruction in POAG or PG. For example, in POAG, the plaque concentration is increased approximately 20% over that

in age-matched normal subjects (Fig 3); a 20% increase in the plaque fraction of the NL group (0.143 increasing to 0.172) would decrease the gel-filled spaces of this group by only 6.5% (0.441 decreasing to 0.412) and would increase flow resistance by this same insignificant fraction. Thus, while the plaque material may be indicative of underlying disease, it is not in itself responsible for the elevated flow resistance characteristic of POAG.

CONCLUSION

The results indicate that the development of the glaucomatous condition in PG and in POAG does not involve a major reduction in the proportion of highly conducting pathways within the JXT. However, it is important to point out that some minor effects are discernible. It is still conceivable that the increase in flow resistance is due to indirect effects of melanin or other substances that have altered the physicochemical properties of the JXT and that were not considered in our models. However, one cannot dismiss the possibility a priori that the JXT generates only a small fraction of the total flow resistance and the glaucomatous condition arises due to alteration in other tissues or by other mechanisms. At any rate, it is fair to end by stating that "the pathogenesis of pigmentary glaucoma is still far from clear"[30] and that it is likely to be more complex than a simple obstruction of aqueous outflow due to pigment.

This study was supported in part by grants EY 02068 and EY 08835 (Dr Alvarado) and EY 05503 (to Roger D. Kamm, Massachusetts Institute of Technology, Cambridge) from the National Eye Institute, National Institutes of Health, Bethesda, Md; The Peter McBean Fund, and That Man May See Inc, San Francisco, Calif; and Research to Prevent Blindness Inc, New York, NY.

Specimens 0169 and 0186 were supplied courtesy of Dunbar Hoskins, MD, and John Hetherington, MD, and specimen 0845, courtesy of Stacy Mettier, Jr, MD, San Francisco; and specimen 0619, courtesy of Martha Luckenbach, MD, Department of Ophthalmology, University of Texas, Dallas.

References

1. Grant WM. Experimental aqueous perfusion in enucleated human eyes. *Arch Ophthalmol.* 1963; 69:783-801.

2. Petersen HR. Can pigmentary deposits on the trabecular meshwork increase the resistance of the aqueous outflow? *Acta Ophthalmol.* 1969;47:743-749.

3. Bellows A, Jocson V, Sears M. Iris pigment granule obstruction of the aqueous outflow channels in enucleated monkey eyes. Presented at the Association for Research in Vision and Ophthalmology Annual Meeting; April 26, 1974; Sarasota, Fla.

4. Epstein DL, Freddo TF, Anderson PJ, Patterson MM, Bassett-Chu S. Experimental obstruction to aqueous outflow by pigment particles in living monkeys. *Invest Ophthalmol Vis Sci.* 1986;27:387-395.

5. Kristensen P. Mydriasis-induced pigment liberation in the anterior chamber associated with acute rise in intraocular pressure in open-angle glaucoma. *Acta Ophthalmol.* 1965;43:714-724.

6. Schenker HI, Luntz MH, Kels B, Podos SM. Exercise-induced increase of intraocular pressure in the pigmentary dispersion syndrome. *Am J Ophthalmol.* 1980;89:598-600.

7. Mapstone R. Pigment release. *Br J Ophthalmol.* 1981;65:258-263.

8. Johnson AT, Alward WLM, Haynes WL. Topical pilocarpine inhibits exercise-induced pigment dispersion in the pigment dispersion syndrome. *Invest Ophthalmol Vis Sci.* 1990;31 (suppl):150.

9. Duncan TE. Pigmentary glaucoma. In: Cairns JE, ed. *Glaucoma.* New York, NY: Grune & Stratton; 1986;2:690.

10. Rodrigues M, Spaeth G, Weinreb S, Sivalingham E. Spectrum of trabecular pigmentation in open-angle glaucoma: a clinicopathologic study. *Trans Am Acad Ophthalmol Otolaryngol.* 1976; 81:258-276.

11. Richardson T, Hutchinson B, Grant W. The outflow tract in pigmentary glaucoma: a light and electron microscopy study. *Arch Ophthalmol.* 1977;95:1015-1025.

12. Benedikt O, Roll P. Elektronenmikroskopische Untersuchungen des Trabekelwerkes bei Pigmentglaukom. *Klin Monatsbl Augenheilkd.* 1980;176:122-130.

13. Kampik A, Green W, Quigley H. Scanning and transmission electron microscopic studies of two cases of pigment dispersion syndrome. *Am J Ophthalmol.* 1981;91:573-587.

14. Richardson T. Pigmentary glaucoma. In: Shields MB, ed. *The Secondary Glaucomas.* St Louis, Mo: Mosby–Year Book; 1982:84-98.

15. Rohen JW, Lütjen-Drecoll E. Morphology of aqueous outflow pathways in normal and glaucomatous eyes. In: Ritch R, Shields MB, Krupin T, eds. *The Glaucomas.* St Louis, Mo: Mosby–Year Book; 1989:41-74.

16. Richardson T. Pigmentary glaucoma. In: Ritch R, Shields MB, Krupin T, eds. *The Glaucomas.* St Louis, Mo: Mosby–Year Book; 1989:981-995.

17. Ethier C, Kamm R, Palazewski B. Calculations of flow resistance in the juxtacanalicular meshwork. *Invest Ophthalmol Vis Sci.* 1986;127: 1741-1750.

18. Seiler T, Wollensak J. The resistance of the trabecular meshwork to aqueous humor outflow. *Graefes Arch Clin Exp Ophthalmol.* 1985;223: 88-91.

19. Alvarado J, Yun A, Murphy C. Juxtacanalicular tissue in primary open angle glaucoma and in nonglaucomatous normals. *Arch Ophthalmol.* 1986;104:1517-1528.

20. Johnson M, Johnson D, Kamm R, DeKater A, Epstein D. The filtration characteristics of the aqueous outflow system. *Exp Eye Res.* 1990;50: 407-418.

21. Shirato S, Murphy CG, Bloom E, et al. Kinetics of phagocytosis in trabecular meshwork cells: flow cytometry and morphometry. *Invest Ophthalmol Vis Sci.* 1989;30:2499-2511.

22. McEwen W. Application of Poiseuille's law to aqueous outflow. *Arch Ophthalmol.* 1958; 60:290-294.

23. Allingham RR, de Kater AW, Ethier CR. Morphometric analysis of Schlemm's canal in normal and glaucomatous human eyes. *Invest Ophthalmol Vis Sci Suppl.* 1991;32:788.

24. Hogan MJ, Alvarado JA, Weddell J. *Histology of the Human Eye: An Atlas and Textbook.* Philadelphia, Pa: WB Saunders Co; 1975:87, 95.

25. Rohen JW, Witmer MD, Fletcher RC. The anatomic basis for glaucoma. *Ann Ophthalmol.* 1978;10:397-411.

26. Rohen JW, Lütjen-Drecoll E. Biology of the trabecular meshwork. In: Lütjen-Drecoll E, ed. *Basic Aspects of Glaucoma Research.* New York, NY: Schattauer; 1982:141-164.

27. Rohen JG. Why is intraocular pressure elevated in chronic simple glaucoma? *Ophthalmology.* 1983;90:758-765.

28. Lütjen-Drecoll E, Futa R, Rohen JW. Ultrahistochemical studies on tangential sections of the trabecular meshwork in normal and glaucomatous eyes. *Invest Ophthalmol Vis Sci.* 1981; 21:563-266.

29. Lütjen-Drecoll E, Shimizu T, Rohrbach MJ, Rohen JW. Quantitative evaluation of 'plaque material' in the inner and outer wall of Schlemm's canal and the ciliary muscle tips in normal and glaucomatous eyes. *Invest Ophthalmol Vis Sci Suppl.* 1984;25:121.

30. Epstein DL. *Chandler and Grant's Glaucoma.* 3rd ed. Philadelphia, Pa: Lea & Febiger; 1986:207.

Printed and Published in the United States of America